Journal of Chromatography A 1728 (2024) 465017

Contents lists available at ScienceDirect

Journal of Chromatography A

journal homepage: www.elsevier.com/locate/chroma

Volatile organic compounds produced during postmortem processes can be linked via chromatographic profiles to individual postmortem bacterial species

Kyle Furuta [a], Julianne Byrne [a], Kawailani Luat [b], Cynthia Cheung [a], David O. Carter [c], Laura Tipton [b,d], Katelynn A. Perrault Uptmor [a,e,*]

[a] Laboratory of Forensic and Bioanalytical Chemistry, School of Natural Sciences and Mathematics, Chaminade University of Honolulu, United States
[b] School of Natural Sciences and Mathematics, Chaminade University of Honolulu, United States
[c] Laboratory of Forensic Taphonomy, School of Natural Sciences and Mathematics, Chaminade University of Honolulu, United States
[d] Departments of Biology and Mathematics & Statistics, James Madison University, United States
[e] Nontargeted Separations Laboratory, Department of Chemistry, William & Mary, United States

ARTICLE INFO

Keywords:
Forensic taphonomy
Decomposition odor
Postmortem microbiology
GC×GC
Forensic chemometrics
Ordination

ABSTRACT

Decomposition odor is produced during postmortem mammalian tissue breakdown by bacteria, insects, and intrinsic chemical processes. Past research has not thoroughly investigated which volatile organic compounds (VOCs) can be linked directly to individual bacterial species on decomposing remains. The purpose of this study was to profile the VOCs produced over time by individual species of bacteria using comprehensive two-dimensional gas chromatography (GC×GC) to expand our foundational knowledge of what each bacterial species contributes to decomposition odor. Five different species of bacteria (*Bacillus subtilis, Ignatzschineria indica, Ignatzschineria ureiclastica, Curtobacterium luteum,* and *Vagococcus lutrae*) were cultured on standard nutrient agar individually and monitored daily using solid phase microextraction arrow (SPME Arrow) and GC×GC in combination with quadrupole mass spectrometry (qMS) and flame ionization detection (FID). The GC×GC-qMS/FID approach was used to generate rich VOC profiles that represented the bacterial species' metabolic VOC production longitudinally. The data obtained from the chromatographic output was used to compare with a prior study using one-dimensional GC-qMS, and also between each of the five species to investigate the extent of overlap between species. No single VOC could be found in all five bacterial species investigated, and there was little overlap in the profile between species. To further visualize these differences, chromatographic peak data was investigated using two different ordination strategies, principal component analysis (PCA) and principal coordinate analysis (PCoA). The two ordination strategies were compared with each other using a Procrustes analysis. This was performed to understand differences in ordination strategies between the separation science community and chemical ecological community. Overall, ordination strategies were found to produce similar results, as evidenced by the correlation of PCA and PCoA in the Procrustes analysis. All analysis strategies yielded distinct VOC profiles for each species. Further study of additional species will support understanding of the holistic view of decomposition odor from a chemical ecology perspective, and further support our understanding of the production of decomposition odor that culminates from such a complex environment.

1. Introduction

Volatile organic compounds (VOCs) have high vapor pressure at room temperature which allows them to evaporate or sublimate and enter the surrounding environment. This class of compounds has vast probative potential in forensic science because they are associated with several types of physical evidence, such as accelerants, drugs, currency, and decomposing remains. For example, scent detection canines, which are trained to search for specific odors, have been extensively used to detect chemical traces from various types of contraband [1], enabling the discovery of forensic evidence for testing and presentation in legal proceedings. VOCs associated with decomposing remains are currently

* Corresponding author at: Department of Chemistry, William & Mary, 540 Landrum Dr, Williamsburg, VA 23185, United States.
E-mail address: kaperrault@wm.edu (K.A. Perrault Uptmor).

https://doi.org/10.1016/j.chroma.2024.465017
Received 10 April 2024; Received in revised form 20 May 2024; Accepted 21 May 2024
Available online 22 May 2024

of particular interest because they have been proposed as having potential to aid medicolegal death investigations [2]. Decomposition odor has been exploited in some studies and cases as a forensic trace. Its presence has the potential to demonstrate the prior location of decomposing remains [3–7]. The core VOCs in decomposition odor have also been shown to change predictably over time, thus presenting the possibility to further develop this forensic trace as a biochemical marker to estimate postmortem interval [8–10]. The ability of physical evidence to provide both spatial and temporal insight into past events is relatively rare, as most physical evidence typically provides one or the other, so forensic traces which provide both insights can be particularly valuable to cases.

Relatively little is known about the origin and biodegradation processes of postmortem VOCs, as this field has only been under study since 2004 [11]. Decomposition VOCs are produced by the biochemical breakdown of tissue macromolecules by enzymes, microbial activity, or environmental degradation [2,12]. There is growing evidence to support that many decomposition VOCs are directly released by metabolic processes of decomposer microorganisms including as bacteria. There is also increasing interest in the study of postmortem microorganisms and the information they can contribute to medicolegal death investigations [13]. These microbes represent a major component of the postmortem food web because they contribute directly to the decomposition of remains [14] and help to attract other decomposers, such as insects, to decomposing remains [15].

Despite the growing need to understand the link between postmortem bacterial species and VOC detection [16], there have been very few studies that investigate postmortem bacteria and VOCs simultaneously [17–19]. Other microbiological research has demonstrated that the direct profiling of metabolic VOC byproducts of bacteria expanded their understanding of VOC signatures and vice versa. For example, the progress towards linking VOCs from pathogens for disease detection, monitoring, and prevention has been synthesized from a large body of literature evolving over the last decade [20–23].

Increasing foundational information on the link between postmortem bacteria and postmortem VOCs may serve to strengthen the ability to exploit decomposition VOCs as a forensic trace. There are several anticipated benefits to improving the knowledge of VOCs released from individual microorganisms or the community in which they are interacting. VOCs may give an indication of the presence or absence of specific bacterial species within a microbial community [24]. VOCs may serve as indicators of the behavior and life cycle of bacteria, including how these are impacted by interaction with other species. A more comprehensive understanding of postmortem bacteria and the VOCs they release could contribute substantial knowledge to the field and has been vastly unexplored.

To profile the VOCs coming from postmortem bacteria, gas chromatography - mass spectrometry (GC–MS) is one of the most appropriate techniques. This involves a chromatographic separation of analytes in the gas phase with subsequent detection using MS to identify and quantify the compounds in the sample. However, in more recent decomposition VOC research, comprehensive two-dimensional gas chromatography (GC×GC) has emerged as a novel tool. The rationale for using a more advanced GC separation is that GC×GC provides a more suitable peak capacity to analyze the complex mixtures of VOCs resulting from decomposition. As the number of VOCs resulting from postmortem bacterial processes is large and complex, GC×GC allows physical separation of each VOC and therefore more accurate integration of peaks of interest. A prior preliminary study using one-dimensional GC–MS (1D GC–MS) demonstrated that 35 compounds of interest were identified from three species of postmortem bacteria [17]. However, there is increased complexity expected in these samples and further analytical resolution would assist in better understanding the complexity of each species and how it relates to the overall decomposition odor profile.

In this study, experiments were conducted to characterize the VOCs released by five postmortem bacterial species cultured in headspace vials and allowed to proliferate over a five-day period. The species studied were *Bacillus subtilis, Ignatzschineria indica, Ignatzschineria ureiclastica, Curtobacterium luteum,* and *Vagococcus lutrae.* While it is known that many more bacterial species are involved in decomposition, this is the greatest number of species to be directly profiled in a single study to date. The data were anticipated to provide a basis for the continued study of other postmortem bacterial species and possible combinations of those species. Species were chosen based on their representation of a range of bacterial characteristics (e.g. shape, Gram stain response), as well as the range in the point in time at which bacteria are known to be present during the decomposition process. More information about each species is discussed alongside the results. The hypothesis in this study was that each species would produce a distinct VOC profile that could be differentiated from one another. The presence of VOCs, number of VOCs, relative abundance of each compound, and overall chemical signature were all considered while testing this hypothesis. Three different ordination strategies (Principal Component Analysis, Principal Coordinate Analysis, and Procrustes Analysis) were employed to visualize VOC profile characteristics for each bacterial species over time.

2. Materials and methods

2.1. Culturing of microbes for headspace analysis

All microbiological preparations were performed in a sterilized laminar flow hood. The growth medium was prepared using 45 g of standard nutrient agar (HiMedia Laboratories Pvt. Ltd., Mumbai, India) in 1 L of deionized water. The agar was mixed, autoclaved, and cooled for 10 min. To prepare the vials, 4 mL of standard nutrient agar was pipetted into each vial and then it was placed on a modified micropipette holder while the agar solidified on a slant. All remaining standard nutrient agar was poured into petri dishes and allowed to cool. Petri dishes and headspace vials were stored at room temperature and left for 3 days before being checked for contamination.

Stock bacteria were taken from an in-house bacteria bank containing various species isolated from decomposing domestic pig carcasses (*Sus scrofa domesticus)*. Bacteria in this collection are stored at −80 °C in glycerol [25]. Three of the species studied (*B. subtilis, I. indica,* and *I. ureiclastica*) represented species previously profiled using GC–MS in a prior study [17] for comparison, while two of the species (*C. luteum, V. lutrae*) have not been studied previously. Samples of each desired species were first thawed and then a sterilized inoculation loop was used to spread an appropriate amount of stock onto the petri dish. Dishes were covered, sealed with parafilm strips, labeled, and stored at room temperature for 1–2 days. The plates were checked for visible colony growth and subcultured onto new plates to remove any remaining glycerol from storage. After three days, bacteria were subcultured from the petri dish into each of three headspace vials while taking care to consistently deliver a uniform bacteria amount to the slanted agar surface. Three of the agar-containing vials were set aside without any inoculated bacteria as blank agar (negative) controls. One autoclaved empty vial without agar was used as a method blank. This resulted in seven samples for each species: three with agar inoculated with bacteria, three with agar that did not contain bacteria, and one empty vial. The initial day of culturing into headspace vials was referred to as "Day 0″ for all trials. Analysis was repeated on all seven vials daily until the end of the trial on the fourth day. This resulted in five days of data collection (35 samples per species) for a total of 175 total samples in this study across all five species.

2.2. GC×GC-qMS/FID method

Instrument configuration consisted of a Thermo Scientific Trace 1300 GC/FID and an ISQ 7000 Single Quadrupole Mass Spectrometer

(qMS) fitted with a Triplus RSH Autosampler for sample introduction using SPME Arrow. A carbon wide range/polydimethylsiloxane (CWR/PDMS) SPME Arrow fiber was used (Restek Corporation, Bellefonte, PA). Fiber preconditioning time at the start of each day was 30 min at 270 °C. Each vial was incubated at 30 °C for 30 s with 250 rpm agitation. The fiber was predesorbed for 5 min at 250 °C to prepare it for exposure. The fiber was exposed to the sample for 5 min with 0 rpm in the Heatex stirrer. The needle speed in vial was 20 mm/s. The fiber was desorbed in splitless mode in the GC inlet for 1 min at 250 °C, with an injection depth of 45 mm/s and penetration speed of 35 mm/s. Following injection, the fiber underwent a 1 min post-desorption conditioning at 250 °C. All conditioning was performed in an offline fiber conditioning station with ultra-high purity nitrogen (Airgas, Radnor, PA, USA). Fiber choice, extraction conditions, and desorption conditions were chosen based on prior work with these sample types, and to keep data as comparable as possible with prior work on this matrix [17,26]. The first dimension column was an Rxi-624Sil MS column (30 m × 0.25 mm ID × 1.4 µm film thickness, Restek Corporation) and the second dimension column was a Stabilwax (5 m × 0.25 mm × 0.25 µm film thickness, Restek Corporation). An INSIGHT Reverse Fill/Flush Modulator (SepSolve Analytical, Peterborough, UK) was used with a modulation period of 2.5 s and flush time of 100 ms. The loop dimensions were 0.53 mm ID × 1133 mm with a loop volume of 25 µL. The bleed line dimensions were 5 m × 0.1 mm ID. Ultra-high purity helium (Airgas) was used as the carrier gas. The flow rate in the first dimension column was 1.00 mL/min and the auxiliary gas flow rate for the second dimension was 20.00 mL/min, with a calculated flow rate of 17.9 mL/min in the second dimension. The flow was split between the FID and MS using an unpurged SilFlow GC 3-port splitter (Trajan Scientific and Medical, UK) at approximately 4.5:1 which was maintained constant throughout the run. The GC oven started at 60 °C, was held for 1 min, increased to a final temperature of 250 °C at the rate of 5 °C/min, and held for 6 min. No secondary oven was used on the secondary column. The total run time was 46 min.

The ion source temperature and the transfer line temperature for the qMS were both set to 280 °C. The qMS was operated in electron ionization mode with a scan range from 40 to 300 *m/z*. The total scan time was 0.0241 s, which resulted in an acquisition rate of 41.5 scans/s. This is the maximum acquisition rate for this instrument when using this scan range. The FID was operated with 350 mL/min ultra-zero grade air (Airgas), 40 mL/min ultra-high purity nitrogen as makeup gas (Airgas), and 35 mL/min ultra-high purity hydrogen (Airgas). The temperature of the FID was set at 250 °C. The scan rate of the FID was 120 Hz. Instrument control was performed using Chromeleon V. 7.2.9 (Thermo Scientific).

2.3. Data processing

Data files from the qMS stream were exported from Chromeleon from *.raw format to *.cdf format using a file converter. Files were then imported into ChromSpace software V. 1.4 (SepSolve Analytical Ltd.). Data files from the FID stream were exported in *.cdf format directly and imported into ChromCompare+ *v*. 1.4 (SepSolve Analytical). Prior studies demonstrated the utility and integration of the FID and qMS data streams in combination, and are not discussed herein [27,28]. Data processing was completed using the ChromCompare+ component of the software. First, baseline correction was performed using 0.35 s. In ChromCompare+ method editor, a tile sum method was created for non-target processing of GC×GC data. FID files were used for feature selection in ChromCompare+ and then identifications were made on selected features using the qMS data files within ChromSpace afterwards. Peak detection integration settings used the tile sum algorithm with a $^{1}t_{R}$ window width of 10 s, a $^{1}t_{R}$ overlap of 20 %, a $^{2}t_{R}$ window width of 0.7 s, and a $^{2}t_{R}$ overlap of 20 %. Peak merging integration was set with an overlap of 2 %, correlation of 0.3, tolerance of 2 %, and intensity of 2 %. Fronting and tailing values were set to 2 % for high and low modulation periods (P_M). The peak filter integration settings for absolute minimum peak height, area, and width were set to zero to avoid pre-filtering of features. In the ChromCompare+ sequencer, FID sample files were batch processed as class standard sample types, assigning the method as detailed above.

A ChromCompare+ project was created by importing the processed sequence and sample classes are assigned in project editor with string label types. Feature discovery was used to filter for the top 50 features. A filtered session report containing the discovered features labeled as numbers and their corresponding peak areas aligned to appropriate the sample, was exported into a Microsoft Excel (2016) file (*.xlsx). The top features in this alignment table were tentatively identified by opening qMS contour plots and utilizing the National Institute of Standards and Technology (NIST) 2017 Mass Spectral Library to tentatively identify peaks. Forward match scores over 700, reverse match scores over 700, and relative probability scores were used in assessing the library hitlist. When ambiguous peak identification information was available, retention indices were used to support compound identification choice, in addition to the location the peak was found on the contour plot (for both $^{1}t_{R}$ and $^{2}t_{R}$) due to knowledge of relative size and polarity of the molecule within the contour plot space (i.e. structured chromatogram information). In some cases, peaks were confirmed using an in-house reference standard mix created from individual analytical standards. The list of top 50 features was condensed to include compounds with a reverse match factor (RMF) of 700 or above.

Ordination was performed on the resulting profiles in R statistical software [29]. Microsoft Excel files (*.xlsx) containing the components of interest and their measurements for each sample were read into R. Principal Components Analysis (PCA) was performed on each bacterial species in base R. Principal Coordinates Analysis (PCoA) and Procrustes were performed on each microbe using the *vegan* R package [30]. Procrustes was used to rotate one ordination to maximize similarity with another ordination; PCA was rotated to maximize similarity with PCoA. PCA, PCoA, and the combination resulting from Procrustes were plotted in R with varying shades of pink for the microbes and cyan for the controls, both getting darker as the sampling day increased.

3. Results and discussion

3.1. Sample and method considerations

To add accurate and reliable information to the foundational knowledge in this field, it is first important to identify the preferred analytical tools for the analysis. Especially in the scenario where a larger database of microbial VOC information may be developed over time, the analytical method must consider all peaks that could be encountered in future studies of individual and combined microorganism studies. In this study, VOC profiling was conducted on three species previously studied by the authors (*B. subtilis, I. indica, I. ureiclastica*) using one-dimensional GC–MS [17]. The other two species studied (*C. luteum* and *V. lutrae*) were investigated to expand the current knowledge based on additional postmortem microorganisms. This initial database therefore includes microbial VOC data for five postmortem microorganisms, all analyzed across the same workflow.

It should be noted that very little information is currently available on four of five of these species (i.e. all but *B. subtilis*) in terms of their impact on the decomposition process, as well as the volatiles produced by them under the conditions presented by outdoor terrestrial decomposition. For reference, a comparison table of the species is presented below demonstrating the variety in species selected for the study (Table 1). All microorganisms chosen for study were Biosafety Level 1 organisms.

Given that three of these species have been previously analyzed using 1D GC–MS, one goal was to evaluate the GC×GC-qMS/FID analysis approach by comparing data from both instruments. Fig. 1 demonstrates the total ion current chromatogram from 1D GC–MS for *I. ureiclastica* alongside the total ion current contour plot from the

Table 1
Species characteristics for chosen bacteria in this study.

Species	Shape	Type of Respiration	Gram Stain	Spore Forming
Bacillus subtilis	Rod	Facultatively anaerobic	Positive	Yes
Ignatzschineria indica	Rod	Aerobic	Negative	No
Ignatzschineria ureiclastica	Rod	Aerobic	Negative	No
Curtobacterium luteum	Rod	Aerobic	Positive	No
Vagococcus lutrae	Coccus	Facultatively anaerobic	Positive	Yes

corresponding GC×GC-qMS data stream. The 1D GC–MS chromatograms demonstrate several regions of peak congestion, for example in the 14–16 min range and the 21–23 min range. The peaks are more fully resolved in the corresponding GC×GC-qMS contour plots, providing improved baseline resolution between peaks and separation from chemical noise in the chromatogram. Prior studies using GC×GC analysis for decomposition odor have highlighted some of these major benefits when performing analyses [31], which results in a more refined resulting peak list due to the improved ability to detect individual components and small changes in amount between these components. It should further be noted when interpreting Fig. 1 and additional supplementary plots in Fig. A1 for each bacterial species, that two different systems were used to acquire these data. There is a major difference in the 2D system whereby the flow modulator is introducing a significantly different amount of flow to the detector, specifically for the mass spectrometer. As such, major components do not necessarily align along the first dimension retention time. The side-by-side comparison is meant to allow a general comparison of peak co-elution and use of chromatographic peak capacity for each method. This is in contrary to other 2D studies where 1D vs. 2D comparisons get performed by simply turning the modulator off, to maintain first dimension retention time comparability. This study refers to a 1D GC–MS system in which no GC×GC components were installed, thus the 1D retention times cannot be compared in a one-to-one fashion.

In this study, the Chromcompare+ software afforded the newer ability to incorporate tile-based Fisher ratio feature selection. This process compares signal intensity between and within classes of samples using a tile sum method. Using this tool, it is possible that some features originally identified manually in 1D GC–MS may not be selected as being peaks of interest as they do not vary significantly between our control group (blank agar) and the treatment group (cultured bacteria) in the GC×GC data. This approach reduces features only to those which are the most effective class differentiators and thereby takes a complex, convoluted chromatogram and allows focus on peaks with the most meaning. In the case of *I. ureiclastica* (Fig. 1), a higher number of peaks of interest were identified by this method. In 1D GC peak identification, 19 peaks were identified as peaks of interest [17]. However, by the GC×GC-qMS/FID workflow incorporating tile-based Fisher ratio feature selection, there were 25 compounds selected as class differentiating features. It is important to note that the second list of features will not

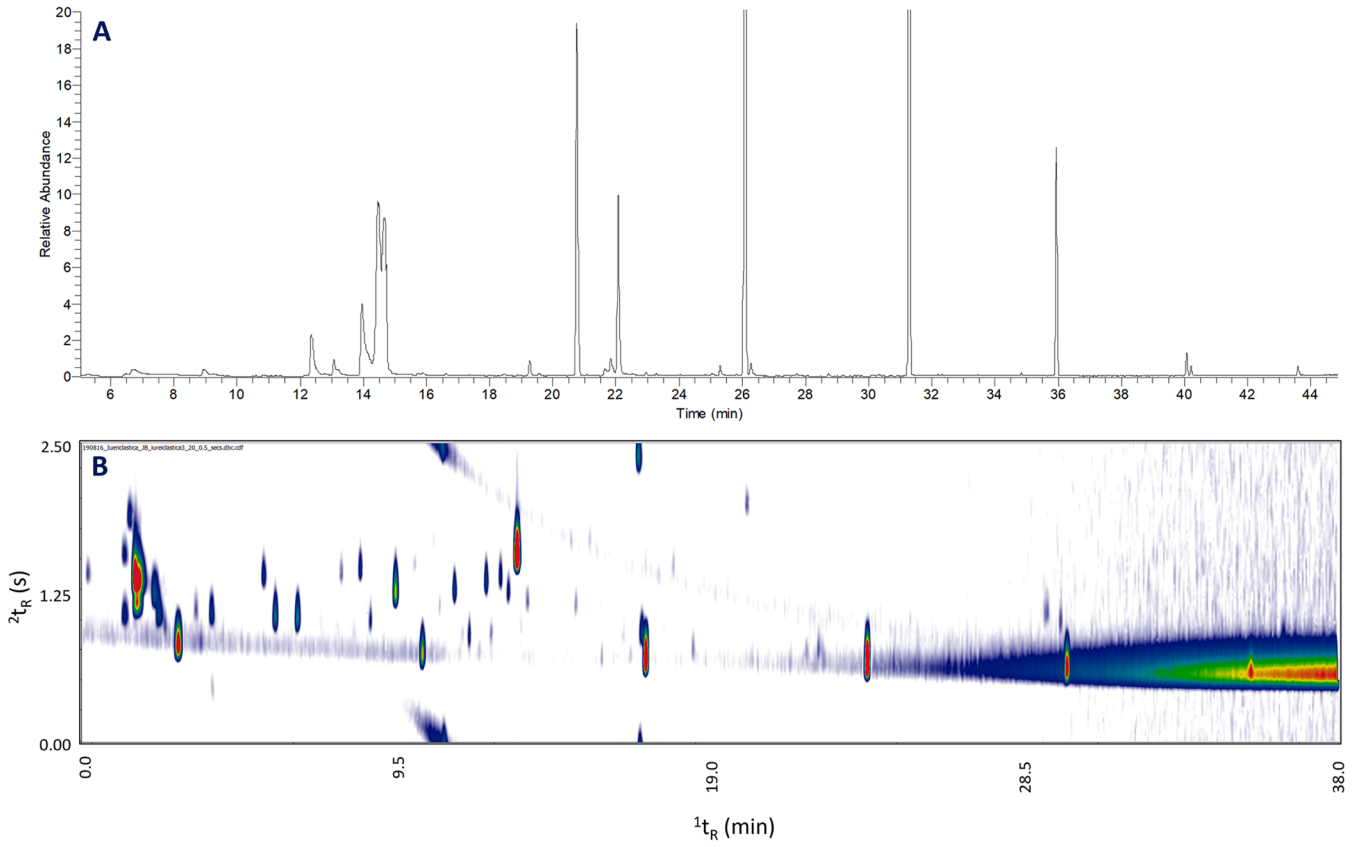

Fig. 1. Total ion current chromatograms for *Ignatzchineria ureiclastica* on Day 4 of analysis using (a) gas chromatography – mass spectrometry and (b) comprehensive two-dimensional gas chromatography – mass spectrometry. The top figure is taken from data collected in [17]. Both chromatograms are zoomed to a portion of the run time to highlight trace level features in further detail. Comparative plots for all three species profiled by both techniques are available in the Supplementary Information, Fig. A1.

always include the 1D GC–MS peaks of interest, since the tile-based Fisher ratio method is generally considered to be more effective in discerning class differentiating compounds [32,33].

The reduction in peak coelution and isolation of individual compound peak areas via physical separation with GC×GC indeed allows a more effective focus on peaks that achieve class characterization (i.e. blank agar vs. bacteria sample). It is also possible however, that the data from a GC×GC analysis will return a list with fewer compounds since chemical noise has been removed resulting in reduced between-class variation. For example, in the prior study, 21 VOCs were initially identified from *I. indica*, yet in this study only eight VOCs were included during feature selection. This occurred even though far greater peaks were identified within the GC×GC-qMS/FID analysis compared to the GC–MS analysis. The increased separation power and peak capacity of GC×GC is especially effective when analyzing samples with a high number of background compounds present in the sample matrix, for example the standard nutrient agar that was used as a matrix in this study. While this advanced analytical technique is useful for this study of individual bacterial species, it also provides promise for future studies where combination of bacterial species is targeted and a mixture of VOC signatures from each combined species must be monitored with even higher complexity.

3.2. VOC profile association with species

In this study, 55 total compounds were identified through feature selection across the five bacterial species. A comprehensive list of each compound selected for each species is provided in Table 2. It is important to note that all compounds identified in this study have been previously identified in postmortem odor studies from mammalian remains.

In decomposition odor analysis, previous studies have identified that odors resulting from decomposing remains exhibit a consistent core profile despite differences in experiment methodology, geographical location, analysis techniques, etc. [10,16,34–36]. One impactful finding was the lack of consistent core profiles of volatiles across the bacterial species. Fig. 2 depicts how many VOCs were identified in common between each of the five species displayed as a multiple intersection Venn diagram. From this diagram it could be observed that there were no compounds that were found in common between all five species. In addition, there were also very few VOCs found in common between four of the five species studied. The number of compounds held as unique VOCs to one species was the highest value out of the other intersection points shared with other species. While this study certainly does not exhaustively characterize all bacterial species that could be present on decomposing remains, these five species' profiles provide support that individual bacteria appear to have a relatively individualistic signature that contribute only a portion of the overall decomposition odor profile, which is a detail that has not been previously established in any decomposition odor studies.

Five VOCs were identified as being found most consistently across the different bacterial species, including acetone, dimethyl disulfide, dimethyl trisulfide, 2-pentanone, and 1-butanol. Fig. 3 demonstrates the VOC relative abundance for each species over time. This longitudinal analysis exemplifies that some bacteria appear to experience a peak in the VOC production during early bacterial proliferation. For example, 1-butanol peaked on Day 1 of the study for *C. luteum*. Dimethyl disulfide also peaked on Day 1 of the study for *V. lutrae*. However, some VOCs appeared to be consistently produced at a steady rate across the study. For example, dimethyl disulfide was observed to be present at a relatively consistent level for *B. subtilis, I. indica,* and *C. luteum* across the life cycle period studied. This is particularly interesting as dimethyl disulfide is one of the most consistently identified compounds in decomposition odor; however, it is also known to oscillate higher and lower over time. The VOC trends observed in prior literature may be explained by different bacterial species establishing themselves at different times throughout the decomposition process. More direct study of species presence alongside VOC data would be required to make these specific linkages.

There were also some cases where one VOC was found in very different levels between the different species. For example, *I. ureiclastica* appeared to produce 2-pentanone at a much lower level than *B. subtilis* or *V. lutrae*. This compound is of specific interest as an early study identified 2-pentanone in high concentrations from human decomposition case studies [37], and it has also been identified from a large number of bacterial species [24]. This data supports that some VOCs detected from decomposing remains may be present from Multiple species contributions, but that in some cases, one or M. species is dominating the contribution of that analyte over other species producing it at lower levels. The GC×GC-FID approach is valuable in these scenarios because it has a broader linear range and therefore should be helpful to characterize analyte differences of larger magnitude in studies such as this. It should be noted that all lines represented in Fig. 3 are measurements that were selected to be different than the VOC trend in blank agar due to the use of the tile-based Fisher ratio feature selection method.

Observing the different temporal trends of individual VOCs may be helpful in better understanding overall decomposition VOC makeup, but pairing bacterial species monitoring with VOC production would drastically improve our understanding of these mechanisms. As few of these multidisciplinary studies have currently been performed in fieldwork trials, the current extrapolation of the bacterial VOC data herein from past studies is limited but still provides promise for linking microbiology and chemistry of human remains. For example, a recent study looked at linking bacteria families with detected VOCs from juvenile pig carcasses [18]. In this study the authors detected dimethyl disulfide at relatively moderate levels across Days 0–4, which also coincided with the detection of Enterococcaceae and Bacillaceae. In our study, *V. lutrae* and *B. subtilis* were found to coincide with this timing and VOC trend for these two families, respectively. While these types of inferences may help to explain trends observed in studies, there is much more research required to specifically pinpoint one individual VOC trend to a group of

Table 2
Full list of VOCs identified after tile-based Fisher ratio feature selection for each species.

Bacillus subtilis	isobutyronitrile, 1,3-pentadiene, 1-butanol, methylene chloride, 2-nitroethanol, acetic acid butyl ester, acetone, acetic acid ethenyl ester, trichloromethane dimethyl trisulfide, 2-pentanone, dimethyl disulfide, pyrrole, 2,5-dimethylpyrazine, 1-chloro-4-trifluoromethylbenzene, methoxyphenyloxime, 4-methylpyrimidine, 3-methylbutanenitrile
Ignatzschineria indica	n-methyltaurine, 2,5-dimethylpyrazine, trimethylpyrazine, 2-heptanone, dimethyl disulfide, 2,4-dimethylpentane, methylpyrazine, benzaldehyde
Ignatzschineria ureiclastica	1-chloro-2-trifluoromethylbenzene, methoxyphenyloxime, benzaldehyde, 2-heptanone, pyrazine, 2-ethyl-5-methylpyrazine, dimethyl trisulfide, 2-methyl-1-propanol, paraldehyde, acetone, acetoin, 3-methylbutanenitrile, methanethiol, 1-chloro-4-trifluoromethylbenzene, 2,6-dimethyl-4-heptanol, propanedioic acid, bromodichloromethane, 4-methyl-2-oxovaleric acid, 3,5-dimethylpyrazine, trichloromethane, 2-pentanone, pyrrole, benzyl alcohol, acetyl valeryl, 3-methylbutanal
Vagococcus lutrae	isoprene, s-methyl 3-methylbutanethioate, 3-methylfuran, 2-butanone, 2-methyl-1-propanol, dimethyl disulfide, 3-methyl-1,5-pentanediol, 4-aminopyridine, 2-pentanone, acetone, 3-methylbutanenitrile, 1-chloro-4-trifluoromethylbenzene, 1,3-diazine, carbon disulfide, methanethiol, 1,2-propanediamine, bromodichloromethane, 1-butanol, dimethyl trisulfide, 5-methyl-2-hexanone, methyl isobutyl ketone
Curtobacterium luteum	3-methyl-2-butanone, S-methylbutanethioic acid, 1-butanol, 2-butanone, acetone, 1-chloro-4-trifluoromethylbenzene, 1,3-butanediol, 3-methylbutanenitrile, methylene chloride, carbamimidothioic acid methyl ester, 1,3-pentadiene, 2-methyl-1-propanol, methylpyrazine, bromodichloromethane, dimethyldisulfide, dimethyltrisulfide, 2,5-dimethylpyrazine, pyrazine, benzyl isopentyl ether

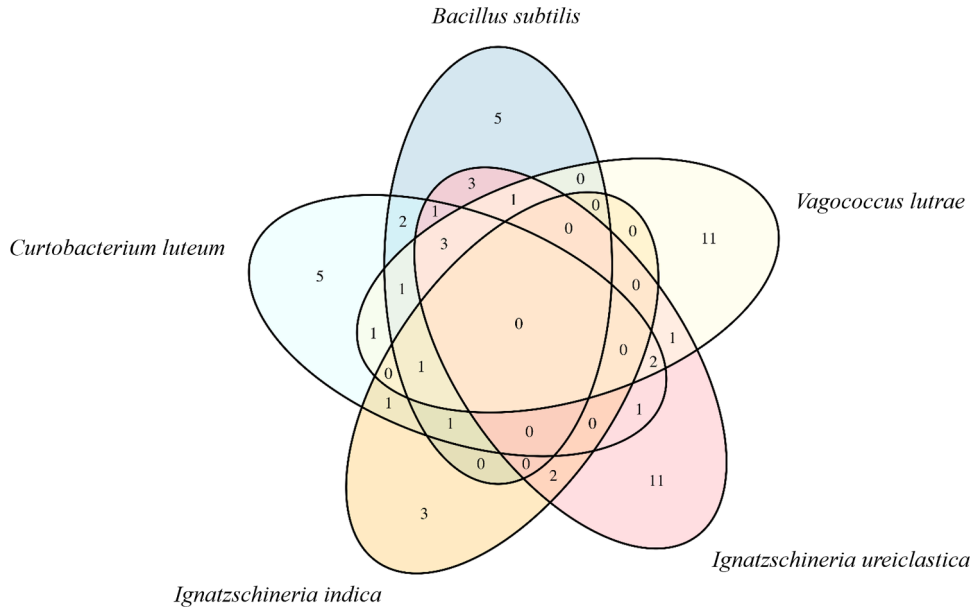

Fig. 2. Multiple intersection Venn diagram showing number of identified compounds for each postmortem bacteria.

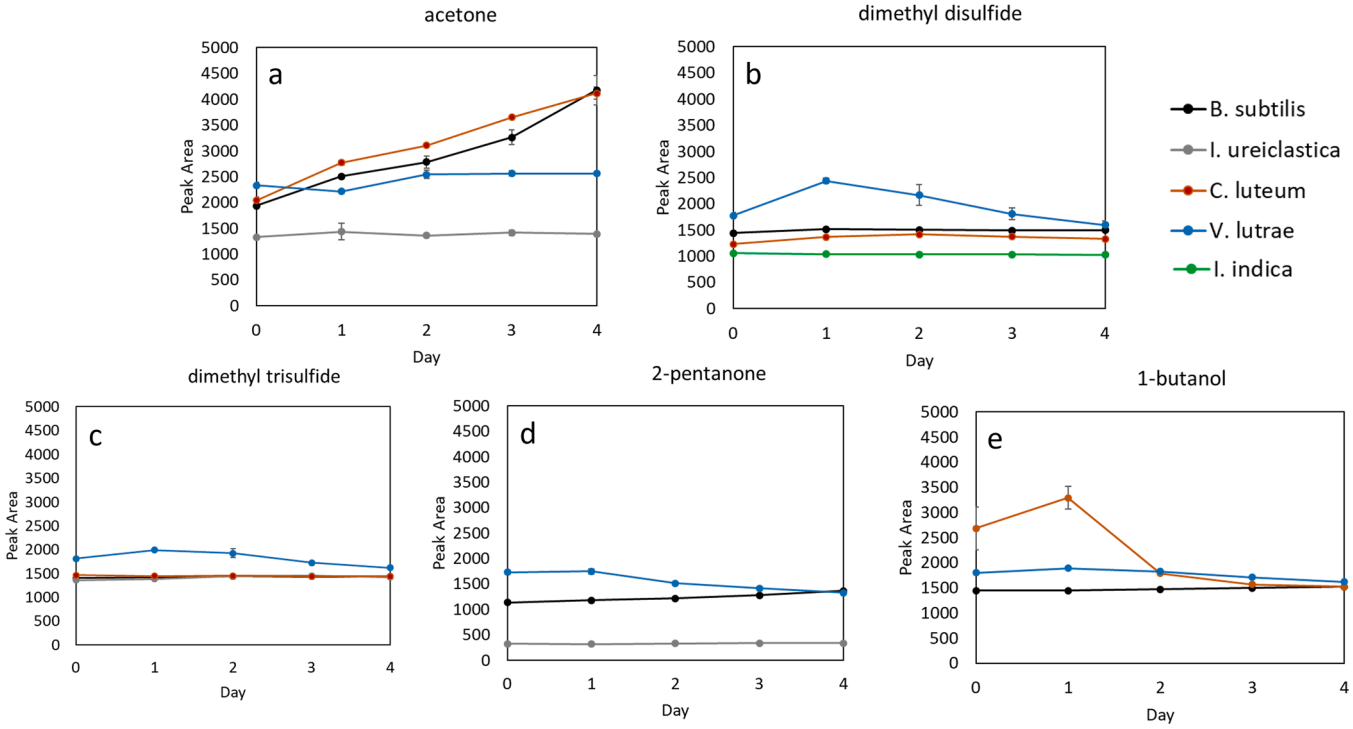

Fig. 3. Line plots demonstrating compound abundance over the days of analysis for 5 common volatile organic compounds (VOCs) identified across bacterial species including (a) acetone, (b) dimethyl disulfide, (c) dimethyl trisulfide, (d) 2-pentanone, (e) 1-butanol.

bacterial species, as would be the case on decomposing remains. Also, as many decomposition ecology studies focus largely on family-level data, it is challenging to link current knowledge of decomposition odor with individual bacterial species without direct laboratory study as presented here.

3.3. Individual species ordination analysis

The investigation of VOCs on an individual basis across different species provides some valuable information as highlighted above. However, because the full chemical fingerprint of all VOCs appeared to be a differentiating factor for each species, examining profile variance more holistically was desirable. Since it was expected that VOC levels would be different depending on different metabolic progress, the visualization of both the presence and abundance of each VOC simultaneously across the full profile is important to understanding how similar or different each bacterial fingerprint may be. As such, visualization through ordination was desired for each species. Ordination is valuable to visualize patterns in a dataset where multiple variables are monitored simultaneously. In the field of GC×GC, the most common ordination approach is Principal Component Analysis (PCA). This technique allows synthetic variables to be produced based on linear

combinations of variables within the dataset. PCA is generally regarded as a valuable visualization tool and exploratory sample comparison technique for multivariate monitoring as it allows the samples to be placed on an ordination plot where distances between samples represent the similarity or dissimilarity of sample profiles. In addition, loadings plots provide explainability of the space between data points on the PCA plot, indicating which specific compounds are driving the similarity or dissimilarity. This has become one of the most popular techniques to visualize GC×GC data to identify unsupervised class differentiation.

However, PCA is confined to measuring similarity or dissimilarity in Euclidean distance, which is not necessarily ideal for profile data. There are multiple reasons for this, including that there is no upper limit to Euclidean distance and therefore two samples with no overlap may not be the greatest distance apart if an additional sample has large values [38]. Additionally, Euclidean distance is not duplicate invariant, so repeating all components will increase the distance between two samples [38]. Finally, it is double zero symmetric, meaning that adding a feature with all zero values is treated the same as adding a value of five for all features, even though the zero may not be real due to variable selection or other measurement artifacts [38]. Principal Coordinate Analysis (PCoA) is another ordination technique commonly used in ecology and microbiome studies. Similarly to PCA, PCoA uses combinations of observed variables to create synthetic variables which can be placed on an ordination plot where distances between the points represent the similarity or dissimilarity of sample profiles, measured with any dissimilarity metric. Bray-Curtis dissimilarity is popular for determining dissimilarities between microbial communities, which share many mathematical properties with VOC profiles. Further information on dissimilarity metrics with example calculations is available in the accompanying Supplementary Information. Bray-Curtis dissimilarity is not a distance but ranges from 0 when two profiles are completely the same to 1 when two profiles are completely different, and the resulting dissimilarity matrix can be readily fed into PCoA. Additionally, the synthetic variables produced by PCoA can be used the same way PCA components are used for multivariate analysis [39], even though the percent of variance explained is not measured in PCoA coordinates. Loading plots are not available for PCoA but biplots can be used to provide the directionality and magnitude of influence of each observed variable. The increased flexibility of using appropriate dissimilarity metrics without the loss of functionality from PCA makes PCoA an ideal technique to visualize GC×GC data to identify unsupervised class differentiation and has not been utilized in GC×GC studies. Most GC×GC data analysis packages currently embed PCA analyses within their program, without considering the appropriateness of this ordination technique compared with other available techniques.

To test the difference between these two ordination techniques on this specific data set, both were applied individually at first, and then forced onto the same plot using a Procrustes analysis. The detailed

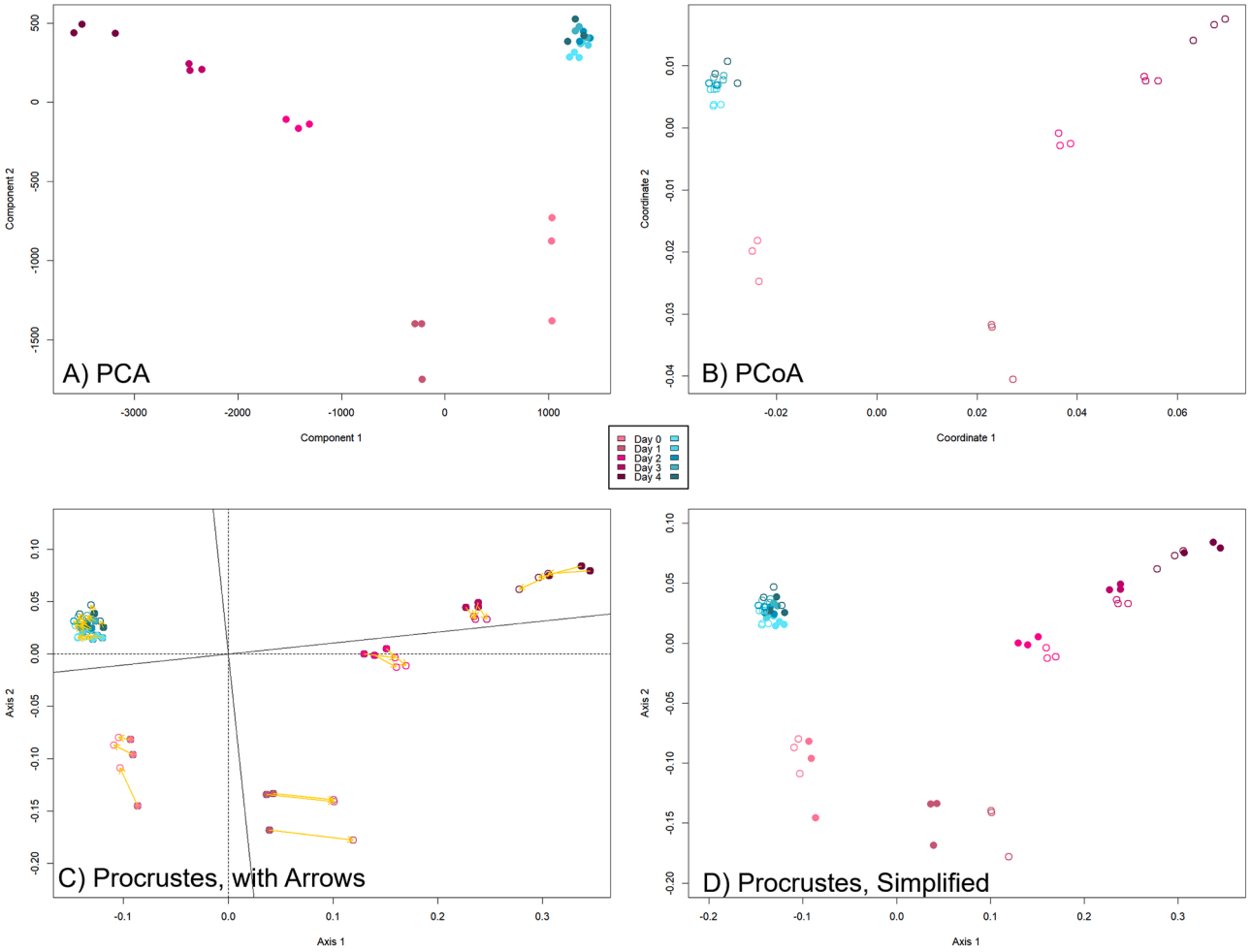

Fig. 4. Ordination plots for *Curtobacterium luteum*. For all plots, the control samples are shown as cyan dots and the microbial samples are shown as maroon dots, both moving from lightest to darkest from Day 0 to Day 4. (A) shows the Principal Component Analysis (PCA) plot based on Euclidean distance; (B) shows the Principal Coordinate Analysis (PCoA) plot based on Bray-Curtis dissimilarity (C) shows the Procrustes plot where the PCA points are in solid circles and the PCoA points are in empty circles. Gold arrows connect the same point from one ordination to the other. Axes are included to show the rotation of the PCA to match the PCoA in addition to the mirroring that occurred. (D) shows a simplified Procrustes plot with the arrows and axes removed.

calculation of Euclidean distance and Bray-Curtis dissimilarity metrics are shown in examples in the Supplementary Information to demonstrate the attributes of each. The Supplementary Information further discusses recent resources for the comparison of PCA and PCoA in Appendix B [38,40]. Procrustes analysis, named from Greek mythology, attempts to rotate and stretch one configuration or matrix to fit as close as possible to another target configuration or matrix. This statistical technique essentially aims at forcing two visualizations to fit one another. The result can be plotted on the same axes as the two matrices will now fall on the same scale, although the scale is meaningless. In addition to calculating rotation, translation of the center, and scaling for plotting, Procrustes analysis measures the correlation between the rotated matrix and the target (non-rotated) matrix as the symmetric sum of squared distances. This statistic can be permuted to determine a *p*-value for significance testing of the correlation between matrices [41], but in general, small sum of squared distances indicate that the two matrices are similar. Unsurprisingly, all pairs of ordination matrices explored here were significantly correlated ($p < 0.0001$) with the sum of squared distances ranging from 0.0253 to 0.6276. Fig. 4 shows the PCA, PCoA, and Procrustes plots for *C. luteum*, which had the smallest sum of squared distances or most similar PCA and PCoA matrices. All bacteria ordination plots can be found in the Supplementary Information Appendix B, Figs. B1–B5. The significant correlation between PCA and PCoA, as well as their visual similarity, highlights that PCoA can be used very similarly to PCA to visually identify unsupervised class differentiation in GC×GC data.

The use of different ordination techniques has proven valuable in many chemometric analyses for multidimensional data, and this study demonstrates an additional application of ordination through PCoA. Further exploration of these techniques on additional data will contribute more information on their utility for different analytical scenarios.

3.4. Limitations

In this study, five different bacterial species were cultured on standard nutrient agar and monitored over a five-day period. However, it is known that a cadaver is a highly complex multispecies environment [42], and therefore the information presented in this study is only a small component of a large network of VOC information that must be studied. It is recommended that many more culturable aerobic bacteria be studied via VOC analysis, as this is the logical next step to improve the linkage between individual species and overall VOC profile. In addition, many VOCs cycle throughout the decomposition process [10,12,34,43], and therefore may be able to be linked with the presence of a specific bacteria on remains at a point in time.

One major consideration in this study is that each bacterial species was treated completely independently of other bacteria that could possibly be in their immediate environment in a real decomposition scenario. In addition, the nutrient agar used in the studied was not varied. It is highly possible that these methodological choices would impact the resulting VOC profile. It is highly recommended that future studies also consider species interactions on standard nutrient agar, in addition to other available growth media.

Lastly, this study focused solely on species that were accessible since they were Biosafety Level 1 (BSL 1) organisms and were able to be cultured under aerobic conditions. To comprehensively understand VOC production by the abundant bacterial species that could be present on decomposing remains, further studies of BSL 2 and anaerobic microorganisms will be necessary.

4. Conclusion

In this study, bacteria that have been previously identified on decomposing remains were investigated using GC×GC-qMS/FID to understand their contribution to decomposition odor. A subset of the bacteria investigated in this study have been previously profiled using GC-qMS, and therefore their profiles could be compared between the two techniques. An additional two species were also profiled in addition to these three repeated species using GC×GC-qMS/FID, and there were no VOCs which were identified across all five species. In addition, the overall profile detected from each bacterial species had minimal overlap with the other species investigated. In an attempt to improve visualization of the highly multivariate data, each species was visualized using both PCA and PCoA ordination strategies. A Procrustes analysis demonstrated that the results of these two strategies were very similar. Key limitations in the structure of data required for PCA suggest that VOC data from GC×GC may be more appropriate to analyze using PCoA rather than PCA, which is a significant divergence from the current state of the field. Further study of VOCs produced by postmortem bacteria could consider species interaction, anaerobic culturing conditions, different growth media, and additional species.

CRediT authorship contribution statement

Kyle Furuta: Writing – review & editing, Writing – original draft, Investigation, Formal analysis. **Julianne Byrne:** Writing – review & editing, Investigation, Formal analysis. **Kawailani Luat:** Writing – review & editing, Visualization, Formal analysis. **Cynthia Cheung:** Writing – original draft, Investigation, Data curation. **David O. Carter:** Writing – review & editing, Supervision, Resources, Methodology, Conceptualization. **Laura Tipton:** Writing – review & editing, Writing – original draft, Visualization, Formal analysis. **Katelynn A. Perrault Uptmor:** Writing – review & editing, Writing – original draft, Visualization, Supervision, Project administration, Methodology, Funding acquisition, Formal analysis, Conceptualization.

Declaration of competing interest

The authors declare the following financial interests/personal relationships which may be considered as potential competing interests:

Katelynn A. Perrault Uptmor reports financial support was provided by National Science Foundation. Katelynn A. Perrault Uptmor reports equipment, drugs, or supplies was provided by Restek Corp. If there are other authors, they declare that they have no known competing financial interests or personal relationships that could have appeared to influence the work reported in this paper.

Data availability

Data will be made available on request.

Funding

This material is based upon work supported by the National Science Foundation under Grant Number 2346598. Any opinions, findings, and conclusions or recommendations expressed in this material are those of the author(s) and do not necessarily reflect the views of the National Science Foundation. The work was further supported by the Henry Dreyfus Teacher Scholar Award from The Camille & Henry Dreyfus Foundation. Funding for project supplies was also supported by the Restek Academic Support Program (RASP) provided by Restek Corporation.

Acknowledgements

The authors would like to thank SepSolve Analytical for support in method and data analysis troubleshooting, as well as Hilary Corcoran from Chaminade University of Honolulu for project and facilities support.

Supplementary materials

Supplementary material associated with this article can be found, in the online version, at doi:10.1016/j.chroma.2024.465017.

References

[1] C. Mesloh, R. Wolf, M. Henych, Scent as forensic evidence and its relationship to the law enforcement canine, J. Forensic Identif. 52 (2002) 169–182.

[2] F. Verheggen, K.A. Perrault, R. Caparros Megido, L.M. Dubois, F. Francis, E. Haubruge, S.L. Forbes, J.F. Focant, P.H. Stefanuto, The odour of death: an overview of current knowledge on characterization and applications, Bioscience 67 (2017) 600–613, https://doi.org/10.1093/biosci/bix046.

[3] L.M. Dubois, P.H. Stefanuto, L. Heudt, J.F. Focant, K.A. Perrault, Characterizing decomposition odor from soil and adipocere samples at a death scene using HS-SPME-GC×GC-HRTOFMS, Forensic Chem. 8 (2018) 11–20, https://doi.org/10.1016/j.forc.2018.01.001.

[4] J. Ensminger, M.A. Ferguson, L.E. Papet, Was there a body in the trunk? Volatile organic compounds in the trial of Casey Anthony and the evolving search for a chemical profile for human decomposition, SMU Sci. Technol. Law Rev. XIX (2016) 275–325.

[5] K.A. Perrault, P.H. Stefanuto, B.H. Stuart, T. Rai, J.F. Focant, S.L. Forbes, Detection of decomposition volatile organic compounds in soil following removal of remains from a surface deposition site, Forensic Sci. Med. Pathol. 11 (2015) 376–387, https://doi.org/10.1007/s12024-015-9693-5.

[6] S.L. Forbes, L. Rust, K. Trebilcock, K.A. Perrault, L.T. McGrath, Effect of age and storage conditions on the volatile organic compound profile of blood, Forensic Sci. Med. Pathol. 10 (2014) 570–582, https://doi.org/10.1007/s12024-014-9610-3.

[7] A.A. Vass, Death is in the air: confirmation of decomposition without a corpse, Forensic Sci. Int. 301 (2019) 149–159, https://doi.org/10.1016/j.forsciint.2019.05.005.

[8] E. Rosier, S. Loix, W. Develter, W. Van de Voorde, J. Tytgat, E. Cuypers, Time-dependent VOC-profile of decomposed human and animal remains in laboratory environment, Forensic Sci. Int. 266 (2016) 164–169, https://doi.org/10.1016/j.forsciint.2016.05.035.

[9] S. Paczkowski, S. Nicke, H. Ziegenhagen, S. Schütz, Volatile emission of decomposing pig carcasses (Sus scrofa domesticus L.) as an indicator for the postmortem interval, J. Forensic Sci. 60 (2015) s130–s137, https://doi.org/10.1111/1556-4029.12638.

[10] S. Stadler, J.P. Desaulniers, S.L. Forbes, Inter-year repeatability study of volatile organic compounds from surface decomposition of human analogues, Int. J. Legal. Med. 129 (2015) 641–650, https://doi.org/10.1007/s00414-014-1024-y.

[11] A.A. Vass, R.R. Smith, C.V. Thompson, M.N. Burnett, D.A. Wolf, J.A. Synstelien, N. Dulgerian, B.A. Eckenrode, Decompositional odor analysis database, J. Forensic Sci. 49 (2004) 760–769. JFS2003434.

[12] H.N. Leblanc, K.A. Perrault, J. Ly, The role of decomposition volatile organic compounds in chemical ecology, J.H. Byrd, J.K. Tomberlin (Eds.). Forensic Entomology: The Utility of Arthropods in Legal Investigations, 3rd ed., CRC Press, Boca Raton, 2019, pp. 485–498.

[13] J.L. Metcalf, Z.Z. Xu, A. Bouslimani, P. Dorrestein, D.O. Carter, R. Knight, Microbiome tools for forensic science, Trends Biotechnol. 35 (2017) 814–823, https://doi.org/10.1016/j.tibtech.2017.03.006.

[14] C.L. Lauber, J.L. Metcalf, K. Keepers, G. Ackermann, D.O. Carter, R. Knight, Vertebrate decomposition is accelerated by soil microbes, Appl. Environ. Microbiol. 80 (2014) 4920–4929, https://doi.org/10.1128/aem.00957-14.

[15] J.K. Tomberlin, T.L. Crippen, A.M. Tarone, M.F.B. Chaudhury, B. Singh, J. A. Cammack, R.P. Meisel, A review of bacterial interactions with blow flies (diptera: calliphoridae) of medical, veterinary, and forensic importance, Ann. Entomol. Soc. Am. 110 (2017) 19–36, https://doi.org/10.1093/aesa/saw086.

[16] S. Paczkowski, S. Schütz, Post-mortem volatiles of vertebrate tissue, Appl. Microbiol. Biotechnol. 91 (2011) 917–935, https://doi.org/10.1007/s00253-011-3417-x.

[17] T. Cernosek, K.E. Eckert, D.O. Carter, K.A. Perrault, Volatile organic compound profiling from postmortem microbes using gas chromatography–mass spectrometry, J. Forensic Sci. 65 (2019) 134–143, https://doi.org/10.1111/1556-4029.14173.

[18] C. Von Hoermann, S. Weithmann, J. Sikorski, O. Nevo, K. Szpila, A. Grzywacz, J. E. Grunwald, F. Reckel, J. Overmann, S. Steiger, M. Ayasse, Linking bacteria, volatiles and insects on carrion: the role of temporal and spatial factors regulating interkingdom communication via volatiles, R. Soc. Open Sci. 9 (2022), https://doi.org/10.1098/rsos.220555.

[19] J. Pascual, C. von Hoermann, A.M. Rottler-Hoermann, O. Nevo, A. Geppert, J. Sikorski, K.J. Huber, S. Steiger, M. Ayasse, J. Overmann, Function of bacterial community dynamics in the formation of cadaveric semiochemicals during *in situ* carcass decomposition, Environ. Microbiol. 19 (2017) 3310–3322, https://doi.org/10.1111/1462-2920.13828.

[20] A. Sharma, R. Kumar, P. Varadwaj, Smelling the disease: diagnostic potential of breath analysis, Mol. Diagn. Ther. 27 (2023) 321–347, https://doi.org/10.1007/s40291-023-00640-7.

[21] A. Abd El Qader, D. Lieberman, Y. Shemer Avni, N. Svobodin, T. Lazarovitch, O. Sagi, Y. Zeiri, Volatile organic compounds generated by cultures of bacteria and viruses associated with respiratory infections, Biomed. Chromatogr. 29 (2015) 1783–1790, https://doi.org/10.1002/bmc.3494.

[22] L.D.J. Bos, P.J. Sterk, M.J. Schultz, Volatile metabolites of pathogens: A systematic review, PLoS Pathog. 9 (2013) e1003311, https://doi.org/10.1371/journal.ppat.1003311.

[23] M.M. Elmassry, B. Piechulla, Volatilomes of bacterial infections in humans, Front. Neurosci. 14 (2020) 257, https://doi.org/10.3389/fnins.2020.00257.

[24] M.C. Lemfack, B.O. Gohlke, S.M.T. Toguem, S. Preissner, B. Piechulla, R. Preissner, MVOC 2.0: A database of microbial volatiles, Nucl. Acids Res. 46 (2018) D1261–D1265, https://doi.org/10.1093/nar/gkx1016.

[25] E.N. Junkins, E.R. Hyde, D.O. Carter, Culture and long-term storage of microorganisms for forensic science, D.O. Carter, J.K. Tomerblin, M.E. Benbow, J. L. Metcalf (Eds.). Forensic Microbiology, Wiley Blackwell, Chichester, UK, 2017, pp. 127–145.

[26] K.E. Eckert, D.O. Carter, K.A. Perrault, Sampling dynamics for volatile organic compounds using headspace solid-phase microextraction arrow for microbiological samples, Separations 5 (2018) 1–15, https://doi.org/10.3390/separations5030045.

[27] L.M. Dubois, S. Aczon, J.F. Focant, K.A. Perrault, Translation of a one-dimensional to a comprehensive two-dimensional gas chromatography method with dual-channel detection for volatile organic compound measurement in forensic applications, Anal. Chem. 92 (2020) 10091–10098, https://doi.org/10.1021/acs.analchem.0c01926.

[28] J.M. Byrne, L.M. Dubois, J.D. Baker, J.F. Focant, K.A. Perrault, A non-targeted data processing workflow for volatile organic compound data acquired using comprehensive two-dimensional gas chromatography with dual channel detection, MethodsX 7 (2020) 101009, https://doi.org/10.1016/j.mex.2020.101009.

[29] R Core Team, R: a language and environment for statistical computing, R Foundation for Statistical Computing (2021) project.org/. https://www.R-project.org/. 2024.

[30] J. Okansen, G. Simpson, F. Blanchet, R. Kindt, P. Legendre, P. Minchin, R. O'Hara, P. Solymos, M. Stevens, E. Szoecs, H. Wagner, M. Barbour, M. Bedward, B. Bolker, D. Borcard, G. Carvalho, M. Chirico, M. De Caceres, S. Durand, A. Evangelist, R. Fitzjohn, M. Friendly, B. Furneax, G. Hannigan, M. Hill, L. Lahti, D. McGlinn, M. Ouellette, E. Ribeiro Cunha, T. Smith, A. Stier, C. Ter Braak, J. Weedon, Vegan: community ecology package, R Package Version 2.6-4 (2022). https://CRAN.R-project.org/package=vegan.

[31] K.A. Perrault, K.D. Nizio, S.L. Forbes, A comparison of one-dimensional and comprehensive two-dimensional gas chromatography for decomposition odour profiling using inter-year replicate field trials, Chromatographia 78 (2015) 1057–1070, https://doi.org/10.1007/s10337-015-2916-9.

[32] L.C. Marney, W.C Siegler, B.A. Parsons, J.C. Hoggard, B.W. Wright, R.E. Synovec, Tile-based Fisher-ratio software for improved feature selection analysis of comprehensive two-dimensional gas chromatography-time-of-flight mass spectrometry data, Talanta 115 (2013) 887–895, https://doi.org/10.1016/j.talanta.2013.06.038.

[33] B.A. Parsons, L.C. Marney, W.C. Siegler, J.C. Hoggard, B.W. Wright, R.E. Synovec, Tile-based Fisher ratio analysis of comprehensive two-dimensional gas chromatography time-of-flight mass spectrometry (GC×GC–TOFMS) data using a null distribution approach, Anal. Chem. 87 (2015) 3812–3819.

[34] L.M. Dubois, D.O. Carter, J.M. Byrne, C. Gutierrez, J.F. Focant, K.A. Perrault, Investigating decomposition odor in a tropical climate by comprehensive two-dimensional gas chromatography (GCxGC) coupled with mass spectrometry (MS) and flame ionization detection (FID), LCGC North Am. 39 (2021) 236–241.

[35] K.A. Perrault, T. Rai, B.H. Stuart, S.L. Forbes, Seasonal comparison of carrion volatiles in decomposition soil using comprehensive two-dimensional gas chromatography - time of flight mass spectrometry, Anal. Methods 7 (2014) 690–698.

[36] S.L. Forbes, K.A. Perrault, P.H. Stefanuto, K.D. Nizio, J.F. Focant, Comparison of the decomposition VOC profile during winter and summer in a moist, mid-latitude (Cfb) climate, PLoS One 9 (2014) e113681, https://doi.org/10.1371/journal.pone.0113681.

[37] M. Statheropoulos, C. Spiliopoulou, A. Agapiou, A study of volatile organic compounds evolved from the decaying human body, Forensic Sci. Int. 153 (2005) 147–155, https://doi.org/10.1016/j.forsciint.2004.08.015.

[38] P. Legendre, M. De Cáceres, Beta diversity as the variance of community data: dissimilarity coefficients and partitioning, Ecol. Lett. 16 (2013) 951–963, https://doi.org/10.1111/ele.12141.

[39] F. Imhann, M. Jan Bonder, A. Vich Vila, J. Fu, Z. Mujagic, L. Vork, E.F. Tigchelaar, S.A. Jankipersadsing, M. Carmen Cenit, H.J.M Harmsen, G. Dijkstra, L. Franke, R. J. Xavier, D. Jonkers, C. Wijmenga, R.K. Weersma, A. Zhernakova, Proton pump inhibitors affect the gut microbiome, Gut Microbiota 65 (2016) 740–748, https://doi.org/10.1136/gutjnl.

[40] J. Debelius, Using PCoA versus PCA, Qiime2forum (2023). https://forum.qiime2.org/t/using-pcoa-versus-pca/26019 (accessed April 2, 2024).

[41] P.R. Peres-Neto, D.A. Jackson, How well do multivariate data sets match? The advantages of a procrustean superimposition approach over the Mantel test, Oecologia 129 (2001) 169–178, https://doi.org/10.1007/s004420100720.

[42] S.J. Finley, M.E. Benbow, G.T. Javan, Microbial communities associated with human decomposition and their potential use as postmortem clocks, Int. J. Legal. Med. 129 (2015) 623–632, https://doi.org/10.1007/s00414-014-1059-0.

[43] C. Brasseur, J. Dekeirsschieter, E.M.J. Schotsmans, S. de Koning, A.S. Wilson, E. Haubruge, J.F. Focant, Comprehensive two-dimensional gas chromatography-time-of-flight mass spectrometry for the forensic study of cadaveric volatile organic compounds released in soil by buried decaying pig carcasses, J. Chromatogr. A 1255 (2012) 163–170, https://doi.org/10.1016/j.chroma.2012.03.048.